JOURNAL OF THERMOPHYSICS AND HEAT TRANSFER
Vol. 12, No. 4, October–December 1998

Local Heat (Mass) Transfer in a Rotating Square Channel with Ejection Holes

C. W. Park,* C. Yoon,† and S. C. Lau‡
Texas A&M University, College Station, Texas 77843-3123

The objective of this experimental investigation was to examine the effects of rotation, flow ejection, channel orientation, and transverse ribs on the local heat (mass) transfer distribution for radial outward flow in a square channel, rotating about a perpendicular axis. The test channel was oriented so that the direction of rotation was perpendicular or at a 45 deg angle to the leading and trailing walls. There were eight ejection holes along the leading or trailing wall of the test channel. The diameter of each ejection hole was equal to one-fifth of the channel hydraulic diameter. The wall with the ejection holes was either smooth or roughened with seven transverse ribs. The ribs were located midway between two ejection holes. The height of the ribs was equal to one-tenth of the channel hydraulic diameter, and the spacing between two ribs was equal to 10 times the rib height. The Reynolds number was 5.5×10^3 and the rotation number range was between 0.0 and 0.24. In a smooth normally oriented channel, rotation in the direction of the ejection flow significantly reduced the local heat/mass transfer on the leading wall, except in the vicinity of the ejection holes. Rotation in a direction opposite to that of the ejection flow widened the high heat/mass transfer regions near the ejection holes on the trailing wall, and reduced the heat/mass transfer in the regions between the ejection holes. In a smooth diagonally oriented channel, the trend of higher heat/mass transfer near the leading side of the leading wall rather than near the trailing side was the opposite of the expected trend for the radial outward flow through a smooth diagonally oriented channel with no ejection holes. Flow reattachment downstream of transverse ribs and flow acceleration toward ejection holes together caused very high heat/mass transfer in bell-shaped regions around the ejection holes. Rotation changed the shape of the local heat/mass transfer distribution more on the leading wall than on the trailing wall of a rib-roughened diagonally oriented channel.

Nomenclature

C_m = cumulative mass of naphthalene in air–naphthalene mixture leaving exit section, kg/s
D = channel hydraulic diameter, m
h_m = local mass transfer coefficient, $\dot{M}''/(\rho_w - \bar{\rho}_b)$, m/s
$\dot{M}''$ = local mass flux of naphthalene, $\rho_s \Delta z/\Delta t$, kg/(m^2 s)
$\dot{m}$ = mass flow rate of air, kg/s
Nu = local Nusselt number
Nu_0 = Nusselt number for fully developed flow, $0.023Re^{0.8}Pr^{0.4}$
Pr = Prandtl number
$\dot{Q}$ = total volumetric flow rate of air that passes through test channel, m^3/s
Re = Reynolds number based on channel hydraulic diameter, $\dot{m}/(\mu D)$
Ro = rotation number, $\Omega D/U$
Sc = Schmidt number of naphthalene in air, $\cong$2.28
Sh = local Sherwood number, $h_m D/\Lambda$
$\overline{Sh}$ = spanwise average Sherwood number
Sh_0 = Sherwood number for fully developed flow, $0.023Re^{0.8}Sc^{0.4}$
U = average air velocity, m/s
X = streamwise distance from inlet of mass transfer active test channel, m
Δt = duration of test run, s
Δz = elevation change of naphthalene surface, m
Λ = diffusion coefficient of naphthalene vapor in air, $0.0681(T/298.16\ \text{K})^{1.93}(1.013 \times 10^5\ \text{Pa}/P_{\text{atm}})$, cm^2/s
μ = dynamic viscosity, N s/m^2
$\bar{\rho}_b$ = average bulk naphthalene vapor density, $0.5(C_m/\dot{Q})$, kg/m^3
ρ_s = density of solid naphthalene, kg/m^3
ρ_w = naphthalene vapor density at wall, kg/m^3
Ω = angular velocity, rad/s

Introduction

IN a coolant passage in a gas turbine blade, the cooling air enters at the base of the blade and exits through film cooling holes along the leading and trailing walls of the channel and through bleed holes at the tip of the blade. Rotational Coriolis and buoyancy forces produce secondary flows throughout the coolant passage. Transverse or skewed rib arrays on the leading and trailing walls force spatially periodic flow separation and reattachment on the opposite walls. Skewed ribs also cause near-wall secondary flows along the directions of the rib axes. In addition, the orientations of the walls with respect to the rotation direction, the irregular cross-sectional shape, and sharp turns (in the case of a serpentine coolant passage) also contribute to the highly complicated flowfield in such a coolant passage. Very large variations of the local heat transfer distributions are expected on the various walls. To be able to identify local hot spots and regions of high thermal stresses in the walls of gas turbine blades, the designer needs sophisticated numerical codes and a substantial experimental database to predict local temperature distributions. This investigation provides experimental results on the effects of flow ejection, channel orientation, and ribs on the local heat transfer distribution for turbulent flow in a rotating channel that models turbine blade internal coolant passages.

Heat transfer literature on turbulent flows in rotating channels with smooth or rib-roughened walls was reviewed in Refs.

Received Nov. 7, 1997; revision received May 28, 1998; accepted for publication June 11, 1998.

*Postdoctoral Associate, Mechanical Engineering Department.
†Graduate Research Assistant, Mechanical Engineering Department.
‡Associate Professor, Mechanical Engineering Department. Member AIAA.

1–3. Wagner et al.[4,5] and Johnson et al.[6,7] investigated the effects of Coriolis and buoyancy forces on the regional average heat transfer in a rotating multipass square channel with smooth walls, and with normal and skewed ribs on the leading and trailing walls. Regional average heat transfer results on the effect of wall temperature variation on the heat transfer in two-pass square channels with smooth walls and with rib-roughened walls were reported.[8–10] Kukreja et al.[1] and Park et al.[2,11] presented local heat/mass transfer distributions on the leading and trailing walls of rotating smooth and rib-roughened two-pass square channels. They also compared their local results with published regional average heat transfer results. The results of these studies showed that, for a radial outward flow, Coriolis forces increased the heat/mass transfer on the trailing wall and decreased that on the leading wall. For a radial inward flow, rotation increased the leading wall heat/mass transfer and decreased the trailing wall heat/mass transfer. The ribs on the leading and trailing walls and the sharp turns reduced the rotation-induced difference between the heat/mass transfer on the two opposite walls.

The effect of flow through ejection holes in a wall on the local heat transfer distribution on the wall for flow through a channel was examined in several studies. Byerley et al.[12,13] presented experimental results on the effects of ejection flow rate and ejection hole inclination angle on the local heat transfer distribution near the entrance to a single ejection hole in one wall of a two-dimensional smooth duct. Byerley et al.[13] also included numerically determined flowfields to help describe the mechanisms responsible for the measured heat transfer distributions. The heat transfer distribution near an ejection hole was dependent on the ejection flow-to-main flow velocity ratio and the inclination angle of the hole. The heat transfer was high near the ejection hole, particularly in a region up to several times the hole diameter downstream of the hole. The heat transfer enhancement upstream of the hole was a result of the local acceleration of the flow entering the hole. Downstream of the hole, the heat transfer enhancement was the result of the redevelopment of the boundary layers, the downwash from a vortex pair, and the local acceleration of the reverse flow immediately downstream of the hole, when the ejection velocity ratio was high.

Shen et al.[14,15] reported the effect of multiple ejection holes and the combined effect of ribs and ejection holes, respectively, on the heat transfer distribution on the wall of a square duct. The flow through an ejection hole was found to reduce the low heat transfer region immediately downstream of a rib and increase the heat transfer near the hole, resulting in an average heat transfer of about 25% over the no ejection hole value.

Ekkad et al.[16] obtained the local heat transfer distributions on the smooth and rib-roughened walls with ejection holes of two-pass square channels. They concluded that, as a result of the increase of the heat transfer near the ejection holes, a total loss of 20–25% of the main flow through the ejection holes did not lower the regional average heat transfer along the channel.

The transient liquid crystal technique was used in the aforementioned experimental studies. Rotational effect was not studied.

In this investigation, naphthalene sublimation experiments are conducted with a rotating square channel with flow ejection holes along the leading or trailing wall. The leading and trailing walls are either smooth or roughened with transverse ribs. The channel is oriented so that the direction of rotation is perpendicular or at a 45 deg angle to the wall with the ejection holes. The analogy between heat and mass transfer is applied to relate mass transfer distributions to heat transfer distributions. Because the maximum variation of the density of the naphthalene vapor–air mixture that flows through the test channel is only about 0.05% of the density of the mixture, buoyancy effect in actual turbine blade coolant passages is not simulated. In addition, to keep the rotation number relatively high to study the effect of rotation, the Reynolds number in this study is lower than that in a typical turbine blade coolant passage.

The naphthalene sublimation technique and the heat and mass transfer analogy have been employed to study local heat transfer in stationary flow passages.[17,18] Goldstein and Cho[19] summarized many of these naphthalene sublimation studies and discussed extensively the analogy between heat transfer and mass transfer.

The experimental results of this investigation will enhance understanding of turbulent heat transfer for flows through rotating channels with ejection holes. The results will also give engine designers detailed local data in the baseline cases of negligible density variation in flows through rotating channels for the validation of their computer codes. These computer codes will be used to predict hot spots and high thermal stress regions in gas turbine blades under actual engine operating conditions. Presently, detailed local data for flows in rotating channels with ejection holes are not available in the open literature.

Experimental Apparatus and Procedure

The test section was a straight channel with a 1.59-cm square cross section, constructed of aluminum (Fig. 1). It was 0.127 m long, equivalent to eight hydraulic diameters. There were eight equally spaced holes of 3.18-mm diameter along one of the walls. That is, the diameter of each hole was equal to one-fifth of the channel hydraulic diameter. Each of the four walls of the test channel was a naphthalene cassette with a shallow cavity on the inner side filled with naphthalene in a casting process. After the walls were assembled, all interior surfaces of the test section were flat, smooth, and mass transfer active.

During an experiment, the test channel rotated with respect to a perpendicular axis (Fig. 1). The channel was oriented so that the wall with the ejection holes was either the leading or trailing wall, and was either normal or at a 45 deg angle to the direction of rotation.

The leading and trailing walls of the test channel were either smooth or roughened with transverse ribs. The other two side walls were smooth walls. Along the rib-roughened channel, seven ribs, cut from square balsa wood strips, were attached with epoxy on the leading and trailing walls. Each rib was located halfway between two ejection holes along the wall with the ejection holes. The rib arrays on the two opposite walls were aligned. The height of the ribs was one-tenth the

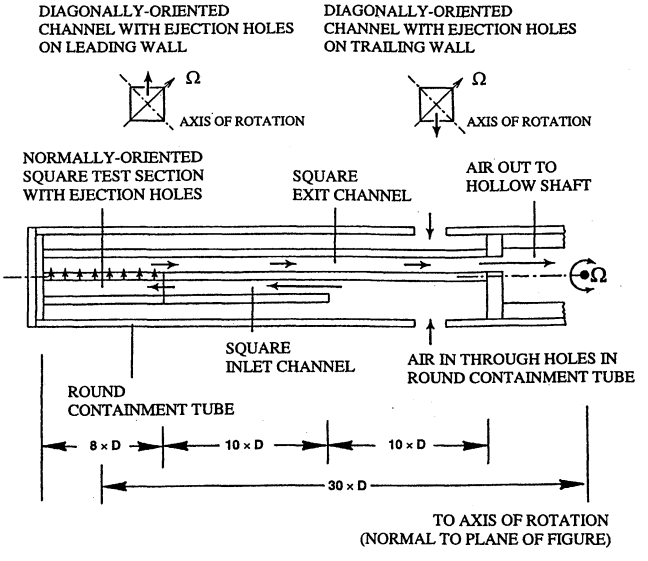

Fig. 1 Schematic of test section, inlet section, and exit section.

channel hydraulic diameter. The spacing between ribs was equal to the hydraulic diameter of the test channel. The exposed surfaces of the ribs were also coated with naphthalene.

Air was drawn radially outward through a 10-hydraulic-diameter long, mass transfer inactive, square entrance channel before entering the test channel. The air then exited through the eight holes along the leading or trailing wall into an 18-hydraulic-diameter long, mass transfer inactive, square downstream channel. Both the entrance and downstream channels had the same cross section as the test channel. The test channel and the downstream channel were parallel to each other and shared the wall with the eight holes. The outer ends of the test channel and downstream channel were closed with a tip wall, so that the air that passed through the downstream channel exited through the inner end of the channel.

The downstream end of the exit section was affixed to a rotating pipe assembly of a rotation test rig in a protective cage. The distance from the middle of the test section to the rotating axis was 30 hydraulic diameters. The entire assembly of the test section, inlet section, and exit section could be rotated about an axis that was perpendicular to the rotating shaft.

For this investigation, the average airflow velocity was 5.3 m/s at the test channel inlet and the maximum rotational speed was 770 rpm, corresponding to a Reynolds number of 5.5×10^3 and rotation numbers up to 0.24, respectively.

During an experiment, room temperature air was drawn through the test section from the air-conditioned laboratory. From the test section assembly, the air flowed through an open flow loop, and left the laboratory before dispersing into the open air. A calibrated orifice flow meter was used to determine the air mass flow rate. An electronic depth gauge was used to measure the elevation changes at up to 544 points on the naphthalene surface of the wall with the ejection holes, and an analytic balance determined the overall weight loss from each of the four walls of the test channel.

Data Reduction

The local Sherwood number at each measurement point is defined as

$$Sh = h_m D/\Lambda \tag{1}$$

The local mass transfer coefficient is evaluated as

$$h_m = \dot{M}''/(\rho_w - \bar{\rho}_b) \tag{2}$$

The naphthalene vapor density at the wall, ρ_w, is calculated according to Ambrose et al.[20] The constant naphthalene vapor density value at the channel walls corresponds to the thermal boundary condition of uniform wall temperature.

The average bulk naphthalene vapor density, $\bar{\rho}_b$, is the average of the inlet bulk naphthalene vapor density, which is equal to zero, and the bulk naphthalene vapor density of the air–naphthalene mixture that leaves the exit channel. The latter is calculated as the cumulative rate of mass of naphthalene in the air–naphthalene mixture that leaves the exit channel divided by the total volumetric flow rate of the air that passes through the test channel. The bulk naphthalene vapor density of the air–naphthalene mixture that leaves the exit channel is small compared with the naphthalene vapor density at the wall: $\bar{\rho}_b$ is only up to 4.1 and 5.5% of ρ_w, respectively, in the smooth and ribbed wall cases in this investigation.

In Eq. (1), the diffusion coefficient for naphthalene vapor in air, Λ, is calculated according to Eq. (1) in Goldstein and Cho.[19]

The Sherwood number is normalized by the Sherwood number for a corresponding fully developed flow in a stationary smooth tube, Sh_0. According to the analogy between heat and mass transfer

$$Nu/Nu_0 = Sh/Sh_0 \tag{3}$$

The Reynolds number and the rotation number, Re and Ro, both of which are based on the channel hydraulic diameter, are defined as $\dot{m}/(\mu D)$ and $\Omega D/U$, respectively.

The uncertainties of the naphthalene vapor density at the wall (relative to $\rho_w - \bar{\rho}_b$) and the local mass flux are 5.4 and 4.0%, respectively, whereas those of the hydraulic diameter, the diffusion coefficient, and the bulk vapor density (relative to $\rho_w - \bar{\rho}_b$) are less than 1.0%. Based on the method described in Kline and McClintock,[21] the maximum uncertainty of the Sherwood number is estimated to be 6.8%. The uncertainty of the Reynolds number is found to be 4.8%.

Presentation and Discussion of Results

Local mass transfer distributions are obtained for radial outward flow through a rotating square channel with ejection holes along the leading wall or the trailing wall. The leading and trailing walls are either smooth or roughened with transverse ribs, and are either normally oriented or diagonally oriented with respect to the rotation direction. The Reynolds number is 5.5×10^3, and the rotation numbers studied are 0.0, 0.12, and 0.24.

First, the local mass transfer distributions on the wall with the ejection holes are displayed as filled contour maps. Corresponding local distributions in the normally oriented and diagonally oriented channels are compared and discussed. Note that each contour map is generated with the Sh/Sh_0 values at a grid of up to 544 points using a computer software that does not change the Sh/Sh_0 values at the points. There is no attempt to extend the contour map to the edges of the wall, the edges of the ejection holes, and the ribs, with extrapolated Sh/Sh_0 values.

The regional average Sherwood number ratios, $\overline{Sh/Sh_0}$, along the wall with the ejection holes are then presented. The $\overline{Sh/Sh_0}$ values are for seven regions between X/D = 1.0 and 2.0, 2.0 and 3.0, . . . , and 7.0 and 8.0, and are given at X/D = 1.5, 2.5, 3.5, . . . , and 7.5.

Effects of Flow Ejection and Rotation: Normally Oriented Smooth Channel

Figure 2 demonstrates the effects of flow ejection and rotation on the local mass transfer distribution on the smooth leading or trailing wall of a normally oriented channel, rotating about a perpendicular axis. The local mass transfer distribution in a stationary channel (with Ro = 0.0) provides the reference

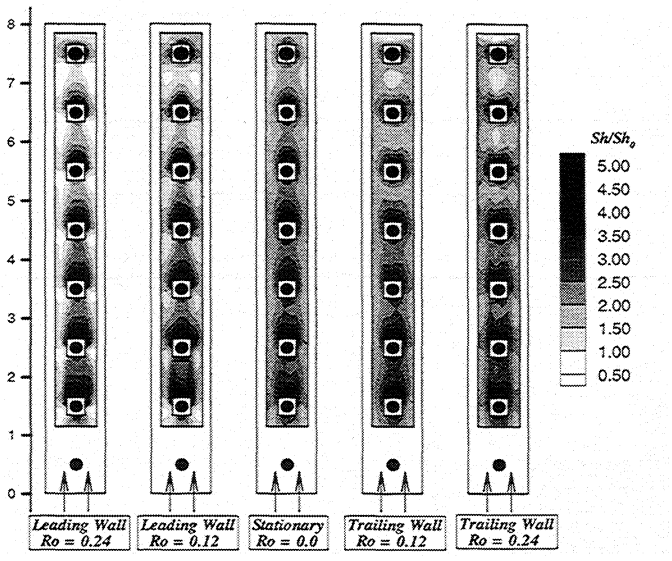

Fig. 2 Sh/Sh_0 distribution on leading or trailing wall with ejection holes in a smooth normally oriented channel ($Re = 5.5 \times 10^3$).

for comparison. With the air exiting through the ejection holes, the local mass transfer is very high near the ejection holes. The local mass transfer is particularly high immediately downstream of the holes, with Sh/Sh_0 values of over 5.0 downstream of most of the ejection holes. The local mass transfer near an ejection hole decreases with distance from the channel entrance. The decrease of the local mass transfer along the channel is particularly evident in the high mass transfer region immediately downstream of an ejection hole. With flow exiting through ejection holes, the airflow rate through the channel decreases along the channel.

The shape of the Sh/Sh_0 distribution around an ejection hole is the result of 1) flow acceleration near the wall immediately upstream of the hole, 2) the redevelopment of the velocity and concentration boundary layers, and 3) the flow being forced toward the wall by a vortex pair downstream of the hole. When the ejection flow rate is very high, the acceleration of a reverse flow entering an ejection hole may also increase the mass transfer immediately downstream of the ejection hole.[13]

In their heat transfer study of flow through a stationary channel with a single ejection hole, Byerley et al.[13] observed a double-lobed heat transfer coefficient distribution downstream of the ejection hole when the ejection flow rate was very high (average hole velocity-to-channel centerline velocity ratio of 7.5) and a single-lobed distribution when the ejection flow rate was low. In this study with multiple ejection holes, the Sh/Sh_0 distributions near all ejection holes in the stationary channel case are single-lobed, with the exception of the distribution near the second ejection hole. Because the distance between consecutive holes in the channel in this study is only five times the diameter of the holes, the Sh/Sh_0 distribution downstream of an ejection hole may be significantly affected by a downstream ejection hole. Note that, in this study, the ratio of the average velocity through the ejection holes to the average velocity at the channel inlet is 3.98.

For radial outward flow in a rotating normally oriented square channel, the rotation-induced Coriolis force pushes the high-momentum core fluid toward the trailing wall. The resulting secondary flow is in the form of two symmetrical vortices. The mass transfer should be higher on the trailing wall and lower on the leading wall, because the high-velocity, low-concentration core flow is shifted toward the trailing wall. When the ejection holes are along the trailing wall of a rotating channel, Coriolis forces act on the wall in the direction of the ejection flow. The Sh/Sh_0 distribution in Fig. 2 shows that rotation increases the mass transfer on the two sides of the ejection holes on the trailing wall. For instance, when $Ro = 0.0$, the Sh/Sh_0 values are as low as 1.5 near the two edges of the wall next to the fifth, sixth, and seventh ejection holes at $X/D = 4.5$, 5.5, and 6.5. When $Ro = 0.12$ and 0.24, the lowest values at those locations are above 1.75 and 2.25, respectively.

Downstream of the fourth ejection hole at $X/D = 3.5$, rotation decreases the mass transfer immediately downstream of the holes on the trailing wall, and in the regions in the middle of the trailing wall between consecutive holes. The shorter high mass transfer regions immediately downstream of the holes with rotation are evident when the Sh/Sh_0 distributions for $Ro = 0.0$, 0.12, and 0.24 are compared. In the $Ro = 0.24$ case, the Sh/Sh_0 values at $X/D = 6.0$ and 7.0 are as low as 1.25 and 1.0, respectively. The mass transfer at these streamwise positions is lower near the middle of the wall and higher along the outer edges of the wall. When there is no rotation, the Sh/Sh_0 values at $X/D = 6.0$ and 7.0 between two holes are above 2.0 and 1.5, respectively, and the mass transfer is higher in the middle of the wall than along the outer edges of the wall. Rotation also decreases the mass transfer downstream of the last ejection hole near the tip wall.

Rotation does not affect the local mass transfer distribution near the second and third ejection holes as much as near the ejection holes farther downstream. Downstream of these two holes, the mass transfer is higher near the middle of the wall and lower near the outer edges of the wall. The trend is reversed gradually farther downstream.

When ejection holes are along the leading wall of a rotating channel, the mass transfer near the ejection holes remains very high downstream of the ejection holes, as in the no-rotation case. The mass transfer, however, is lower near the two outer edges of the wall and between two ejection holes. With no rotation, the lowest Sh/Sh_0 values of between 1.25 and 1.5 are along the two outer edges of the wall near the downstream end of the channel. When $Ro = 0.12$ and 0.24, the lowest Sh/Sh_0 values are below 1.0 and 0.75, respectively, in isolated regions of low local mass transfer near the outer edges of the wall.

Figure 3 presents the effect of rotation on the streamwise variation of the regional average Sherwood number ratio. The regional average mass transfer in all cases generally decreases along the channel. With ejection holes along the trailing wall, rotation increases the mass transfer. On the other hand, with ejection holes along the leading wall, rotation decreases the mass transfer.

Effects of Flow Ejection and Rotation: Diagonally Oriented Smooth Channel

When the channel is oriented at a 45-deg angle with respect to the direction of rotation, Coriolis forces act diagonally across the flow cross section. Figure 4 shows the local mass

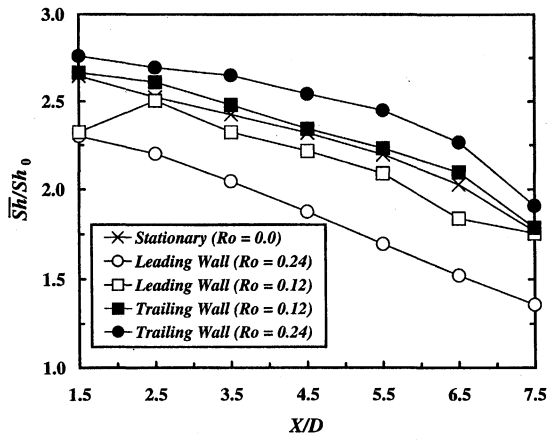

Fig. 3 Streamwise $\overline{Sh}/Sh_0$ distribution on leading or trailing wall with ejection holes in a smooth normally oriented channel.

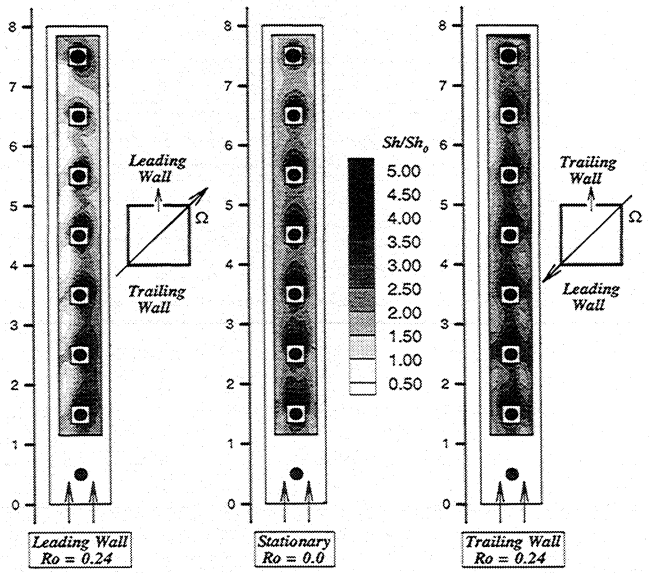

Fig. 4 Sh/Sh_0 distribution on leading or trailing wall with ejection holes in a smooth diagonally oriented channel ($Re = 5.5 \times 10^3$).

transfer distributions on the leading and trailing walls with the ejection holes, along with two sketches (each of which is a top view of the diagonally oriented square channel) that give the direction of rotation relative to the leading and trailing walls. The local mass transfer distribution in the stationary channel case is also included for comparison. Without ejection flow through the holes, rotation-induced secondary flow, which should be symmetrical about a diagonal plane, would cause the mass transfer to be higher on one side (near the trailing edge) of the trailing wall than on the other side of the trailing wall. The mass transfer on the leading wall would also be higher near the trailing edge of the wall than near the leading edge of the wall. The average mass transfer on the trailing wall would be higher than that on the leading wall.

With flow through the ejection holes along the leading wall, Fig. 4 shows that the high mass transfer regions downstream of the holes are shifted toward the leading edge of the wall (the right edge of the leading wall Sh/Sh_0 distribution in the figure). Downstream of the fourth through seventh ejection holes (at X/D = 3.5 and 6.5), the mass transfer in the region immediately downstream of an ejection hole clearly drops faster along the channel than in the stationary channel case. The Sh/Sh_0 values between two ejection holes over the middle of that section of the channel are consistently lower than those in the stationary channel case. The relatively high mass transfer around the last ejection hole on the leading wall of a diagonally oriented channel is very different from the low mass transfer around the last ejection hole in the leading wall of a normally oriented channel (see Fig. 2).

Figure 4 also shows that there are isolated regions of very low mass transfer, with Sh/Sh_0 values about or below 0.75, near the trailing edge of the leading wall (the left side of the leading wall Sh/Sh_0 distribution in the figure). The mass transfer near the leading (or right) edge of the leading wall is higher than that near the trailing (or left) edge. The trend of higher leading wall mass transfer on the leading side than on the trailing side of the wall is the reverse of the expected trend in the case of radial outward flow through a rotating channel without ejection holes.

With ejection holes along the trailing wall, the mass transfer in the region immediately downstream of an ejection hole drops slower along the channel than in the stationary channel case. Thus, the mass transfer between two ejection holes is higher than in the stationary channel case. The high mass transfer regions downstream of the holes are shifted slightly toward the leading (or left) edge of the wall.

The mass transfer is higher on the trailing (or right) side of the trailing wall than on the leading (or left) side. On the trailing (or right) side of the trailing wall, the Sh/Sh_0 value is as high as over 3.0, but is between 1.75 and 2.5 in periodic regions of lower mass transfer. On the leading (or left) side, the Sh/Sh_0 value is as low as below 1.25 near the downstream holes.

Figure 5 gives the streamwise variation of the regional average Sherwood number ratio in a smooth diagonally oriented channel with ejection holes in the leading or trailing wall. Again, rotation increases the mass transfer on the trailing wall, and decreases the mass transfer on the leading wall. The reduced main flow through the channel again causes the regional average mass transfer on both the leading and trailing walls with ejection holes to decrease along the channel, except for the high mass transfer on both walls at the last ejection hole.

For the same total airflow rate and rotational speed (Re = 5.5 × 10^3 and Ro = 0.24), the overall average mass transfer is slightly higher on both the leading and trailing walls of a diagonally oriented channel than on corresponding walls of a normally oriented channel (see Figs. 3 and 5).

Effects of Flow Ejection and Rotation: Normally Oriented Channel with Rib-Roughened Leading and Trailing Walls

Figure 6 presents the effects of flow ejection, transverse ribs, and rotation on the local mass transfer distribution on the leading or trailing wall of a normally oriented channel, rotating about a perpendicular axis. Transverse ribs cause spatially periodic flow separation from the top edges of the ribs and reattachment on the wall downstream of the ribs. The boundary layers on the wall redevelop until the downstream ribs are encountered. Flow ejection through a hole in the middle of the wall midway between two ribs pulls the main flow in the middle of the channel toward the hole and should increase the mass transfer on the wall between two ribs. Rotation-induced Coriolis forces should further increase the mass transfer on the trailing wall, but may reduce that on the leading wall.

In the no-rotation case (see middle of Fig. 6), the local mass transfer is very high in bell-shaped regions on the wall surrounding the ejection holes. As mentioned earlier, the high mass transfer is caused by the flow being pulled toward the holes and flow reattachment downstream of the ribs. It is believed that the slowly recirculating air that would have been trapped immediately downstream of the ribs is pulled toward the holes in the middle of the wall. The mass transfer is thus lower in the middle than near the two edges of the wall immediately downstream of the ribs. The shapes of the local mass transfer distributions are consistent with those of the local heat transfer distributions in Shen et al.[15]

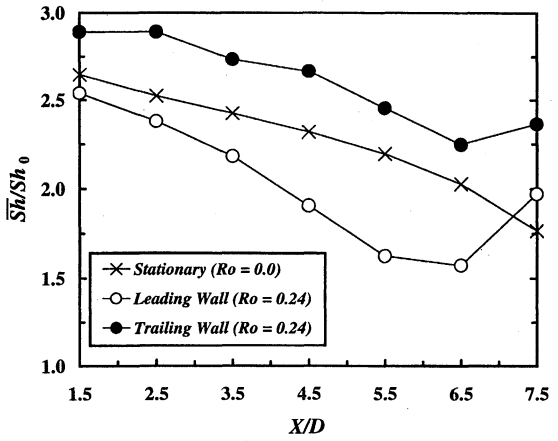

Fig. 5 Streamwise $\overline{Sh}/Sh_0$ distribution on leading or trailing wall with ejection holes in a smooth diagonally oriented channel.

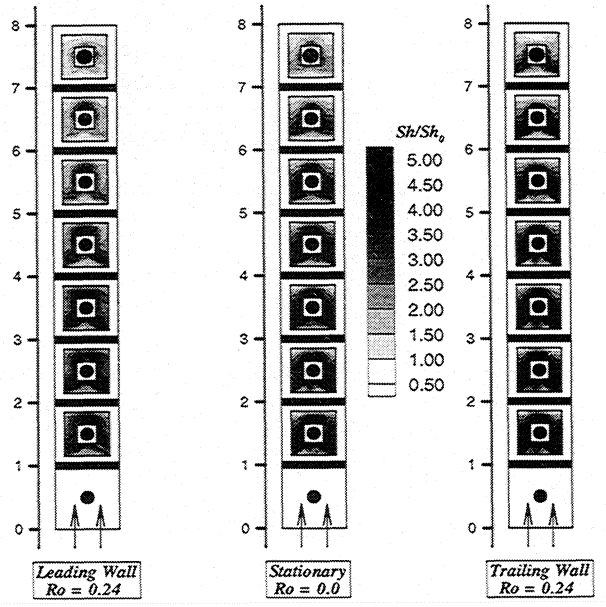

Fig. 6 Sh/Sh_0 distribution on leading or trailing wall with ejection holes in a rib-roughened normally oriented channel (Re = 5.5 × 10^3).

Although the flow through the ejection holes causes high mass transfer immediately downstream of the holes, the mass transfer in the region immediately downstream of an ejection hole decreases faster along the channel than in the smooth wall case. The high mass transfer regions immediately downstream of the ejection holes are shorter in the ribbed wall case than in the smooth wall case. The downstream ribs may force the flow to lift off the wall in the regions between the holes and the downstream ribs. In the smooth wall case, the downstream holes may pull the approaching near-wall flow toward the wall, keeping the mass transfer relatively high in the regions immediately downstream of the ejection holes.

The decreasing airflow rate through the channel again causes the local mass transfer between consecutive ribs to decrease along the channel. Over the first four pitches from the first rib, the Sh/Sh_0 values are about or over 5.0 in the reattachment regions downstream of the ribs and in the vicinity of the ejection holes. Downstream of the last rib, there is only a weak reattachment on the wall, with Sh/Sh_0 values of less than 2.5.

With the channel rotating in the same direction as the ejection flow, the local mass transfer is decreased almost everywhere on the wall with the ejection holes. Rotation-induced Coriolis forces significantly reduce the strength of the reattaching flows downstream of the ribs on the leading wall. Near the two edges of the leading wall, where the influence of the ejection flow may be the smallest, the mass transfer in the boundary-layer redevelopment regions is much lower than in the stationary channel case. Flow reattachment on the leading wall is not evident downstream of the last two ejection holes.

Rotating the channel in a direction opposite to the ejection flow does not significantly change the pattern of the local mass transfer distribution on the wall with the ejection hole. The Sh/Sh_0 distribution up to $X/D = 4.0$ is almost the same as that in the stationary channel case. Beyond the fourth ribs, rotation increases the mass transfer on the trailing wall with the ejection holes, although the pattern of the local distribution remains similar to that in the stationary channel case.

Figure 7 gives the effect of rotation on the distribution of the regional average Sherwood number ratio along the rib-roughened, normally oriented channel with flow ejection through holes along the leading or trailing wall.

Effects of Flow Ejection and Rotation: Diagonally Oriented Channel with Rib-Roughened Leading and Trailing Walls

With the channel oriented diagonally, rotation significantly changes the pattern of the local mass transfer distribution on the leading wall, as shown in Fig. 8. It is difficult to tell where on the wall the separated flow over a rib reattaches, if the separated flow reattaches at all. The Sh/Sh_0 values on the leading (or right) side of the wall are higher than those on the trailing (or left) side of the wall. Overall, the Sh/Sh_0 values on the leading wall are lower than those on the leading wall in the stationary channel case.

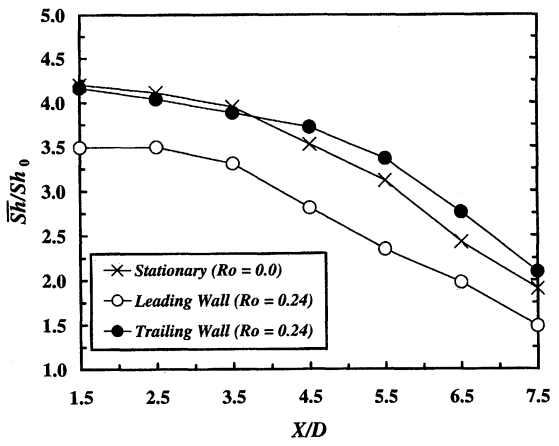

Fig. 7 Streamwise $\overline{Sh}/Sh_0$ distribution on leading or trailing wall with ejection holes in a rib-roughened normally oriented channel.

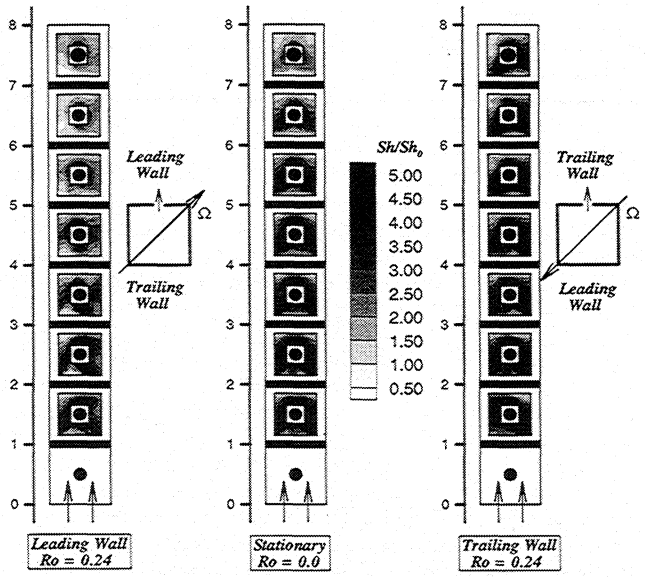

Fig. 8 Sh/Sh_0 distribution on leading or trailing wall with ejection holes in a rib-roughened diagonally oriented channel (Re = 5.5 × 10^3).

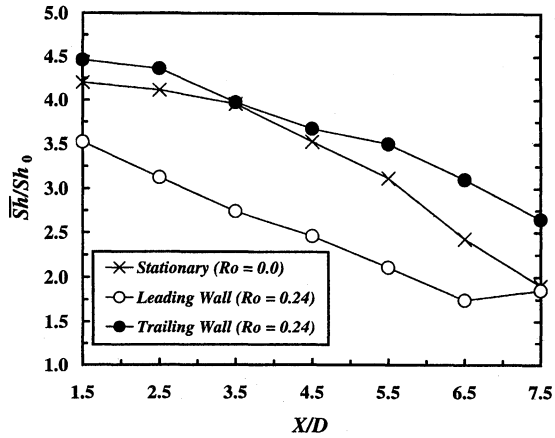

Fig. 9 Streamwise $\overline{Sh}/Sh_0$ distribution on leading or trailing wall with ejection holes in a rib-roughened diagonally oriented channel.

Rotation does not affect the local mass transfer distribution on the trailing wall as much as on the leading wall. The patterns of the distributions on the trailing wall are similar to those in the stationary channel, except that the rotation-induced Coriolis forces appear to keep the mass transfer near the reattachment regions relatively high near the trailing (or right) side of the wall. Downstream of the third rib from the channel entrance, the Sh/Sh_0 values are higher on the trailing (or right) side than on the leading (or left) side of the wall. Near the entrance, the difference between the Sh/Sh_0 values in the left and right halves of the trailing wall may be too small to distinguish.

Figure 9 gives the effect of rotation on the distribution of the regional average Sherwood number ratio along the rib-roughened, diagonally oriented channel with flow ejection through holes along the leading or trailing wall. As expected, rotation again causes the regional average mass transfer to be lower on the leading wall and higher on the trailing wall than in the stationary case.

Conclusions

Naphthalene sublimation experiments have been conducted to determine the effects of ejection holes, channel orientation,

and transverse ribs on the detailed local heat/mass transfer distributions, for turbulent radial outward flow through a rotating square channel with ejection holes along the leading wall or the trailing wall. The channel was either normally oriented or diagonally oriented with respect to the rotation direction. The Reynolds number was 5.5×10^3, and the rotation numbers were between 0.0 and 0.24. Under the conditions of this investigation, the following conclusions may be drawn:

1) Flow through ejection holes significantly increases the local heat/mass transfer near the ejection holes, particularly in the regions immediately downstream of the holes. In a smooth normally oriented channel, rotation in the direction of the ejection flow significantly reduces the local heat/mass transfer on the leading wall, except in the vicinity of the ejection holes. Rotation in a direction opposite to that of the ejection flow widens the high heat/mass transfer regions near the ejection holes on the trailing wall, and reduces the heat/mass transfer in the regions between the ejection holes.

2) In a smooth diagonally oriented channel, flow through ejection holes causes the heat/mass transfer on the leading wall to be higher on the leading side of the wall than on the trailing side. The trend is the opposite of the expected trend for radial outward flow through a smooth diagonally oriented channel with no ejection holes.

3) In a smooth diagonally oriented channel with ejection holes along the trailing wall, rotation increases the heat/mass transfer near the ejection holes, and causes the heat/mass transfer to be higher on the trailing side of the wall than on the leading side, the same as the expected trend in the no-ejection flow case.

4) Flow reattachment downstream of transverse ribs and flow acceleration toward ejection holes together cause very high heat/mass transfer in bell-shaped regions around the ejection holes. Rotation in a normal direction increases the heat/mass transfer on the trailing wall and decreases that on the leading wall, but does not significantly change the bell-shaped high heat/mass transfer regions.

5) In a diagonally oriented channel with rib-roughened walls, rotation changes the shape of the local heat/mass transfer distribution more on the leading wall than on the trailing wall. On the trailing wall, the heat/mass transfer is higher on the trailing side of the wall than on the leading side.

Acknowledgment

The NASA Lewis Research Center, Cleveland, Ohio, sponsored this research, Grant NAG3-1980.

References

[1]Kukreja, R. T., Park, C. W., and Lau, S. C., "Heat (Mass) Transfer Distribution in a Rotating Two-Pass Square Channel—Part II: Local Heat Transfer, Smooth Channel," *International Journal of Rotating Machinery*, Vol. 4, No. 1, 1998, pp. 1–15.

[2]Park, C. W., Kukreja, R. T., and Lau, S. C., "Effect of Rib Size on Heat (Mass) Transfer Distribution in a Rotating Channel," American Society of Mechanical Engineers, Paper 97-AA-126, Sept. 1997.

[3]Tse, D. G. N., and Steuber, G., "Flow in Rotating Serpentine Coolant Passages With Skewed Trip Strips," NASA CR 198530, Oct. 1996.

[4]Wagner, J. H., Johnson, B. V., and Kopper, F. C., "Heat Transfer in Rotating Serpentine Passages With Smooth Walls," *Journal of Turbomachinery*, Vol. 113, July 1991, pp. 321–330.

[5]Wagner, J. H., Johnson, B. V., Graziani, R. A., and Yeh, F. C., "Heat Transfer in Rotating Passages with Trips Normal to the Flow," *Journal of Turbomachinery*, Vol. 114, Oct. 1992, pp. 847–857.

[6]Johnson, B. V., Wagner, J. H., and Steuber, G. D., "Effects of Rotation on Coolant Passage Heat Transfer: Volume II—Coolant Passages with Trips Normal and Skew to the Flow," NASA CR 4396, Oct. 1993.

[7]Johnson, B. V., Wagner, J. H., Steuber, G. D., and Yeh, F. C., "Heat Transfer in Rotating Serpentine Passages with Trips Skewed to the Flow," *Journal of Turbomachinery*, Vol. 116, Jan. 1994, pp. 113–123.

[8]Han, J. C., Zhang, Y. M., and Kalkuehler, K., "Uneven Wall Temperature Effect on Local Heat Transfer in a Rotating Two-Pass Square Channel with Smooth Walls," *Journal of Heat Transfer*, Vol. 115, Nov. 1993, pp. 912–920.

[9]Parson, J. A., Han, J. C., and Zhang, Y. M., "Wall Heating Effect on Local Heat Transfer in a Rotating Two-Pass Square Channel with 90° Rib Turbulators," *International Journal of Heat and Mass Transfer*, Vol. 37, Sept. 1994, pp. 1411–1420.

[10]Zhang, Y. M., Han, J. C., Parsons, J. A., and Lee, C. P., "Surface Heating Effect on Local Heat Transfer in a Rotating Two-Pass Square Channel with 60 Deg Angled Rib Turbulators," *Journal of Turbomachinery*, Vol. 117, April 1995, pp. 272–280.

[11]Park, C. W., Lau, S. C., and Kukreja, R. T., "Heat/Mass Transfer in a Rotating Two-Pass Square Channel with Transverse Ribs," *Journal of Thermophysics and Heat Transfer*, Vol. 12, Jan. 1998, pp. 80–86.

[12]Byerley, A. R., Ireland, P. T., Jones, T. V., and Ashton, S. A., "Detailed Heat Transfer Measurements near and Within the Entrance of a Film Cooling Hole," American Society of Mechanical Engineers, Paper 88-GT-155, 1988.

[13]Byerley, A. R., Jones, T. V., and Ireland, P. T., "Internal Cooling Passage Heat Transfer near the Entrance to a Film Cooling Hole: Experimental and Computational Results," American Society of Mechanical Engineers, Paper 92-GT-241, June 1992.

[14]Shen, J. R., Ireland, P. T., and Jones, T. V., "Heat Transfer Coefficient Enhancement in Gas Turbine Blade Cooling Passage Due to Film Cooling Holes," *Proceedings of Turbomachinery: Latest Developments in a Changing Scene*, Inst. of Mechanical Engineers, London, March 1991, pp. 219–226.

[15]Shen, J. R., Wang, Z., Ireland, P. T., Jones, T. V., and Byerley, A. R., "Heat Transfer Enhancement Within a Turbine Blade Cooling Passage Using Ribs and Combinations of Ribs with Film Cooling Holes," *Journal of Turbomachinery*, Vol. 118, No. 3, 1996, pp. 428–434.

[16]Ekkad, S. V., Huang, Y., and Han, J. C., "Detailed Heat Transfer Distributions in Two-Pass Smooth and Turbulated Square Channels with Bleed Holes," American Society of Mechanical Engineers, HTD-Vol. 330, New York, Aug. 1996, pp. 133–140.

[17]Kukreja, R. T., Lau, S. C., and McMillin, R. D., "Local Heat/Mass Transfer Distribution in a Square Channel with Full and V-Shaped Ribs," *International Journal of Heat and Mass Transfer*, Vol. 36, No. 8, 1993, pp. 2013–2020.

[18]McMillin, R. D., and Lau, S. C., "Effect of Trailing-Edge Ejection on Local Heat (Mass) Transfer in Pin Fin Cooling Channels in Turbine Blades," *Journal of Turbomachinery*, Vol. 116, Jan. 1994, pp. 159–168.

[19]Goldstein, R. J., and Cho, H. H., "A Review of Mass Transfer Measurements Using Naphthalene Sublimation," *Experimental Thermal and Fluid Science*, Vol. 10, May 1995, pp. 416–434.

[20]Ambrose, D., Lawrenson, I. J., and Sprake, C. H. S., "The Vapor Pressure of Naphthalene," *Journal of Chemical Thermodynamics*, Vol. 7, Dec. 1975, pp. 1173–1176.

[21]Kline, S. J., and McClintock, F. A., "Describing Uncertainties in Single Sample Experiments," *Mechanical Engineering*, Vol. 75, Jan. 1953, pp. 3–8.